

# Optimizing Lutetium 177–Anti–Carbonic Anhydrase IX Radioimmunotherapy in an Intraperitoneal Clear Cell Renal Cell Carcinoma Xenograft Model

Constantijn H.J. Muselaers, Egbert Oosterwijk, Desirée L. Bos, Wim J.G. Oyen, Peter F.A. Mulders, and Otto C. Boerman

## Abstract

A new approach in the treatment of clear cell renal carcinoma (ccRCC) is radioimmunotherapy (RIT) using anti–carbonic anhydrase IX (CAIX) antibody G250. To investigate the potential of RIT with lutetium 177 ( $^{177}\text{Lu}$ )-labeled G250, we conducted a protein dose escalation study and subsequently an RIT study in mice with intraperitoneally growing ccRCC lesions. Mice with intraperitoneal xenografts were injected with 1, 3, 10, 30, or 100  $\mu\text{g}$  of G250 labeled with 10 MBq indium 111 ( $^{111}\text{In}$ ) to determine the optimal protein dose. The optimal protein dose determined with imaging and biodistribution studies was used in a subsequent RIT experiment in three groups of 10 mice with intraperitoneal SK-RC-52 tumors. One group received 13 MBq  $^{177}\text{Lu}$ -DOTA-G250, a control group received 13 MBq nonspecific  $^{177}\text{Lu}$ -MOPC21, and the second control group was not treated and received 20 MBq  $^{111}\text{In}$ -DOTA-G250. The optimal G250 protein dose to target ccRCC in this model was 10  $\mu\text{g}$  G250. Treatment with 13 MBq  $^{177}\text{Lu}$ -DOTA-G250 was well tolerated and resulted in significantly prolonged median survival (139 days) compared to controls (49–53 days,  $p = .015$ ), indicating that RIT has potential in this metastatic ccRCC model.

THE APPROVAL OF targeted therapies such as tyrosine kinase inhibitors (TKIs) and inhibitors of mammalian target of rapamycin has revolutionized the treatment of advanced clear cell renal cell carcinoma (ccRCC) during the last decade. Sunitinib, pazopanib, temsirolimus, and bevacizumab in combination with interferon- $\alpha$  have improved progression-free survival and are now approved as first-line treatments for metastatic ccRCC.<sup>1–5</sup> Unfortunately, these agents have several disadvantages. First, they are associated with sometimes severe side effects, such as diarrhea, hypertension, fatigue, and hand-foot syndrome.<sup>6</sup> Moreover, treatment with these drugs is not curative, implicating chronic treatment. In addition, discontinuation of therapy may lead to flare-up of disease activity in some patients.<sup>7</sup> Continued treatment despite disease progression or a switch to another

angiogenesis inhibitor with a relatively short interval is therefore necessary.

The need for a less toxic therapeutic option with good and durable responses led to studies targeting the carbonic anhydrase IX (CAIX) using monoclonal antibody (mAb) G250 (chimeric mAb also known as girentuximab). G250 specifically binds to CAIX, which is expressed in approximately 94% of ccRCCs, and expression in normal tissues is limited.<sup>8</sup> This preferential high expression in ccRCC has been used in many preclinical and clinical studies for imaging and therapy of ccRCC.<sup>9</sup>

Due to the limited efficacy observed in the first clinical trials using  $^{131}\text{I}$ -girentuximab, the search for more suitable radionuclides was initiated. A preclinical study by Brouwers and colleagues revealed the superior therapeutic efficacy of lutetium 177 ( $^{177}\text{Lu}$ )-, yttrium 90-, or rhenium 186-labeled girentuximab compared to iodine 131 ( $^{131}\text{I}$ )-labeled girentuximab. As tumor growth in mice with subcutaneous xenografts was delayed most effectively by the  $^{177}\text{Lu}$ -labeled antibody,<sup>10</sup> a phase I dose escalation trial with  $^{177}\text{Lu}$ -girentuximab in patients with advanced ccRCC was initiated. The results of this trial were very promising as  $^{177}\text{Lu}$ -girentuximab radioimmunotherapy (RIT) was generally well tolerated and resulted in disease stabilization in the majority of patients.<sup>11</sup> However, now the question

From the Departments of Urology and Nuclear Medicine, Radboud University Medical Center, Nijmegen, The Netherlands.

Address reprint requests to: Constantijn H.J. Muselaers, MD, Departments of Urology and Nuclear Medicine, Radboud University Medical Center, Geert Grooteplein Centraal 10, 6525 GA Nijmegen, The Netherlands; e-mail: [stijn.muselaers@radboudumc.nl](mailto:stijn.muselaers@radboudumc.nl).

DOI 10.2310/7290.2014.00008

© 2014 Decker Intellectual Properties

DECKER

arises as to how to combine RIT with other treatment modalities, such as TKIs, as we recently found that the uptake of girentuximab is markedly reduced during treatment with these agents.<sup>12</sup> To design the optimal treatment strategy, additional preclinical studies regarding the sequencing of therapies are of the utmost importance.

In preclinical studies to date, tumor growth was induced by subcutaneous injection of tumor cells or grafting of harvested xenograft tissue, resulting in a single, palpable, visible tumor.<sup>10,13</sup> Although the growth of subcutaneous tumors can be monitored easily with caliper measurements, subcutaneously growing xenografts differ substantially from tumor lesions in patients, particularly with respect to blood supply and physiology.<sup>14,15</sup> In this study, we evaluated the potential of combined radio-immunodetection and RIT with murine G250 in an intraperitoneal ccRCC xenograft model that may more closely mimic human metastatic ccRCC.

## Materials and Methods

### Antibodies

G250 is a murine IgG1 mAb that is directed against the CAIX antigen expressed in ccRCC. The G250 antibody was affinity purified on a Protein-A column from the supernatant of G250 hybridoma cell cultures. MOPC21 (Sigma-Aldrich, Zwijndrecht, The Netherlands) is a murine IgG1 mAb not directed against any known antigen and was used as a negative control in the RIT experiment.

### Conjugation, Radiolabeling, and Quality Control

For the antibody dose escalation study, both G250 and MOPC21 were conjugated with isothiocyanato-benzyl-diethylenetriaminepentaacetic acid (ITC-DTPA), as described previously.<sup>10</sup>

For biodistribution studies, DTPA-conjugated G250 was incubated with <sup>111</sup>In (Covidien BV, Petten, The Netherlands) in 0.1 M MES buffer, pH 5.5, at room temperature, under strict metal-free conditions for 20 minutes as described previously.<sup>16</sup> The specific activity of the antibody preparation was 1.07 MBq/μg (yield 98%). The protein dose was adjusted to 3, 10, 30, or 100 μg by adding unlabeled G250. For single-photon emission computed tomography (SPECT)/computed tomography (CT) studies, 67.2 μg DTPA-conjugated G250 was incubated with 403 MBq <sup>111</sup>In. This preparation was purified on a PD10 column. The specific activity of <sup>111</sup>In-DTPA-G250 used for imaging studies was 3.4 MBq/μg (overall yield 19%). Again,

the protein dose for the different groups was adjusted by adding unlabeled G250. Ten megabecquerels of <sup>111</sup>In-DTPA-G250 was administered intravenously via the tail vein (0.2 mL).

For the therapy experiment, isothiocyanato-benzyl-1,4,7,10-tetraazacyclododecanetetraacetic acid (ITC-DOTA) was used as a bifunctional chelator because of the slightly better stability with <sup>177</sup>Lu.<sup>10</sup> DOTA conjugation was performed essentially as described by Lewis and colleagues.<sup>17</sup> No-carrier-added <sup>177</sup>Lu was acquired from ITG (Garching, Germany). For RIT, antibody-DOTA conjugates were radiolabeled with <sup>177</sup>Lu (G250: 46% yield, MOPC21 53% yield) or with <sup>111</sup>In (74% yield). The radiochemical purity of the radiolabeled antibody preparations in the RIT experiment all exceeded 95%. The specific activity of <sup>177</sup>Lu-DOTA-G250, <sup>177</sup>Lu-DOTA-MOPC21, and <sup>111</sup>In-DOTA-G250 was 1.3, 1.3, and 1.6 MBq/μg, respectively.

### Cell Culture

Tumor growth was induced by an intraperitoneal injection of 0.2 mL of a suspension of  $3 \times 10^6$  SK-RC-52 cells, a CAIX-expressing human ccRCC cell line,<sup>18</sup> resulting in tumor nodules (submillimeter to 3 mm in diameter) in the peritoneal cavity after 2 to 4 weeks.

### Animals

All experiments were conducted in accordance with the principles laid out by the revised Dutch Act on Animal Experimentation (1997) and approved by the institutional Animal Welfare Committee of the Radboud University Nijmegen. Animals were housed and fed according to the Dutch animal welfare regulations. The experiments were performed in female nude BALB/c nu/nu mice (8–10 weeks old) weighing 20 to 25 g (Janvier, le Genest-Saint-Isle, France). Mice were accustomed to laboratory conditions for at least 1 week before experimental use and housed under nonsterile standard conditions in filter-topped cages with free access to animal chow and water.

### Protein Dose Escalation Study

Twenty-five female athymic BALB/c nu/nu mice were injected with SK-RC-52 cells as described above and divided in five groups. Three weeks after inoculation, the mice were injected with 3, 10, 30, or 100 μg G250-DTPA labeled with 10 MBq <sup>111</sup>In. At the 1 μg dose level, the protein dose was too low for labeling with activity doses required for SPECT imaging. Therefore, the conjugate in this group was labeled

with 1 MBq only, which is sufficient to determine the biodistribution of the radiolabeled antibody.

Imaging with the U-SPECT II scanner (MILabs, Utrecht, The Netherlands) was performed in the 3, 10, 30, or 100  $\mu\text{g}$  groups 48 hours postinjection of  $^{111}\text{In}$ -DTPA-G250. A 1.0 mm diameter pinhole collimator tube was used. Mice were anesthetized with a mixture of oxygen,  $\text{N}_2\text{O}$ , and isoflurane and placed in a supine position in the scanner. Body temperature was maintained at  $38^\circ\text{C}$  during the scan. The total scan time was approximately 60 minutes per animal for SPECT acquisition and 3 minutes for CT imaging. Images were reconstructed using the MILabs software. Immediately after completion of image acquisition, mice were euthanized, and the intraperitoneal cavity was inspected meticulously for the presence of intraperitoneal tumor depositions. Tumor nodules and tissues were dissected, and their concentration of the radiolabel (%ID/g) was determined. If no tumor lesions were detected, animals were excluded from the ex vivo biodistribution studies.

A tumor sample and samples of normal tissues (blood, muscle, heart, lung, spleen, pancreas, stomach, duodenum, kidney, liver) were dissected, weighed, and counted in a gamma counter (1480 Wizard 3, LKB/Wallace, Perkin-Elmer, Boston, MA). Injection standards were also counted to correct for radioactive decay. Tissue uptake of the radiolabeled antibody was expressed as a percentage of the injected dose per gram (%ID/g).

### RIT Experiment

For the RIT experiment, 30 female BALB/c nu/nu mice were injected with SK-RC-52 cells as described and divided into three groups. Two weeks after tumor cell inoculation, mice were injected with 10  $\mu\text{g}$  13 MBq  $^{177}\text{Lu}$ -DOTA-G250 ( $n = 10$ ), 13 MBq  $^{177}\text{Lu}$ -DOTA-MOPC21 (control group,  $n = 10$ ), or 20 MBq  $^{111}\text{In}$ -DOTA-G250 (control group,  $n = 10$ ).

The weight of the mice was measured weekly, and mice were euthanized in case of excessive palpable tumor growth, substantial weight loss, or other signs of significant disease progression, as determined by trained biotechnicians who were blinded for the treatment given to the mice. As in the protein dose escalation study, the presence of intraperitoneal tumor depositions was scored macroscopically. Animals were excluded from survival analyses if no tumor lesions were detected after inspection of the abdomen. SPECT/CT imaging to monitor disease progression was performed at 3-week intervals as described above. Primary end points were overall survival and toxicity.

### Statistical Analysis

Statistical analyses were performed using IBM SPSS Statistics version 20.0 (IBM, Armonk, NY) and GraphPad Prism version 5.03 (GraphPad Software, San Diego, CA). Differences in uptake of radiolabeled antibodies were tested for significance using the nonparametric Kruskal-Wallis test and were considered significant at  $p < .05$ , two-sided. Tumor to blood (T/B) ratios were calculated by averaging the T/B ratios of the individual animals (tumor uptake [%ID/g] divided by blood activity [%ID/g]). Values are expressed as mean  $\pm$  standard deviation. Median survival differences were tested for significance using a Mantel-Cox test and were considered significant at  $p < .05$ .

## Results

### Protein Dose Escalation Study

Mice did not show clinical signs of discomfort 3 weeks after inoculation of the SK-RC-52 tumor cells. At that time, the intraperitoneal tumor nodules were not palpable. On macroscopic inspection of the opened abdomen, multiple solid tumors were found, predominantly located at the subhepatic, -splenic, and -phrenic spaces and within the mesentery (Figure 1). The number of tumor lesions per mouse was typically more than 10, ranging in diameter from less than a millimeter to 3 mm. Eighteen of 25 mice (72%) had macroscopically visible tumors at dissection. Mice without macroscopically visible tumor growth were excluded from analyses.

SPECT/CT imaging showed high mAb uptake in the abdomen of mice at all protein dose levels. No clear differences in image quality were observed between the

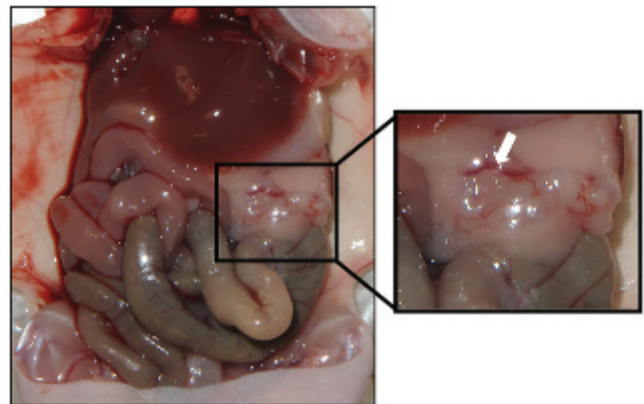


**Figure 1.** Intraperitoneal tumor depositions close to the pancreas and spleen 21 days after tumor cell inoculation. Note the extensive neovascularization surrounding the tumors (arrow).

different groups. After the animals were sacrificed, all imaged areas coincided with intraperitoneal tumors, which ranged from 1 to 2 mm, demonstrating preferential mAb uptake in the tumors. The biodistribution of  $^{111}\text{In}$ -DTPA-G250 was determined 48 hours postinjection (Figure 2). Tumor uptake of the radiolabeled antibody was very high at all protein dose levels, with the highest mean uptake observed in the 10  $\mu\text{g}$  group ( $54.9 \pm 3.5$ ), but the difference between the groups was not significant.

The highest T/B ratio was found in the 1  $\mu\text{g}$  group ( $14.7 \pm 11.6$ ), mainly due to lower blood values, but the ratio was not statistically significant different from that of the other groups ( $p = .297$ ). Significantly higher liver uptake was observed in the 3  $\mu\text{g}$  group ( $23.0 \pm 9.5$ ) compared to the 10, 30, and 100  $\mu\text{g}$  dose level groups ( $p = .036$ ). At protein dose levels  $\geq 10 \mu\text{g}$ , favorable T/B ratios ( $8.5 \pm 3.3$ ,  $5.1 \pm 1.8$  and  $4.4 \pm 1.1$ , respectively) and lower liver uptake was observed, especially in the 10  $\mu\text{g}$  group (T/B ratio  $8.5 \pm 3.3$ ). Therefore, it was concluded that the optimal G250 dose to target ccRCC in this model was 10  $\mu\text{g}$ .

### RIT Study

Twenty-nine of 30 mice (97%) developed visible tumors during the experiment as assessed by meticulous macroscopic inspection of the peritoneal cavity. All mice survived the treatment, and apart from mild transient weight loss ( $< 15\%$ ) associated with the  $^{177}\text{Lu}$ -labeled

antibody preparations, treatment was generally well tolerated. Three mice died during the imaging procedures (injections or anesthesia) and were excluded from the analyses. One of these animals did not have macroscopically visible tumor growth.

Survival curves of the three groups are shown in Figure 3. Mice reached the humane end point when signs of significant disease progression or clinical deterioration (mainly severe weight loss) occurred, as judged by blinded biotechnicians. Lesion size ranged from  $< 1.0$  to 12 mm. The response to treatment was also monitored with  $^{111}\text{In}$ -DTPA-G250 SPECT/CT. As shown in Figure 4, the progression of tumor lesions could easily be monitored in vivo, and when animals were sacrificed, a close correlation between SPECT images and macroscopic tumors was observed.

Treatment with  $^{177}\text{Lu}$ -DOTA-G250 resulted in significantly prolonged median survival of 139 days, which is significantly longer than the survival of the mice in both control groups. The median survival of the mice that received  $^{177}\text{Lu}$ -DOTA-MOPC21 was 49 days and 53 days in the  $^{111}\text{In}$ -DOTA-G250-treated group (Mantel-Cox test,  $p = .015$ ). The study was terminated after 150 days, the preset end point for assessment of survival.

### Discussion

In this study, the potential of radioimmunodetection and RIT with radiolabeled G250 in an intraperitoneal ccRCC

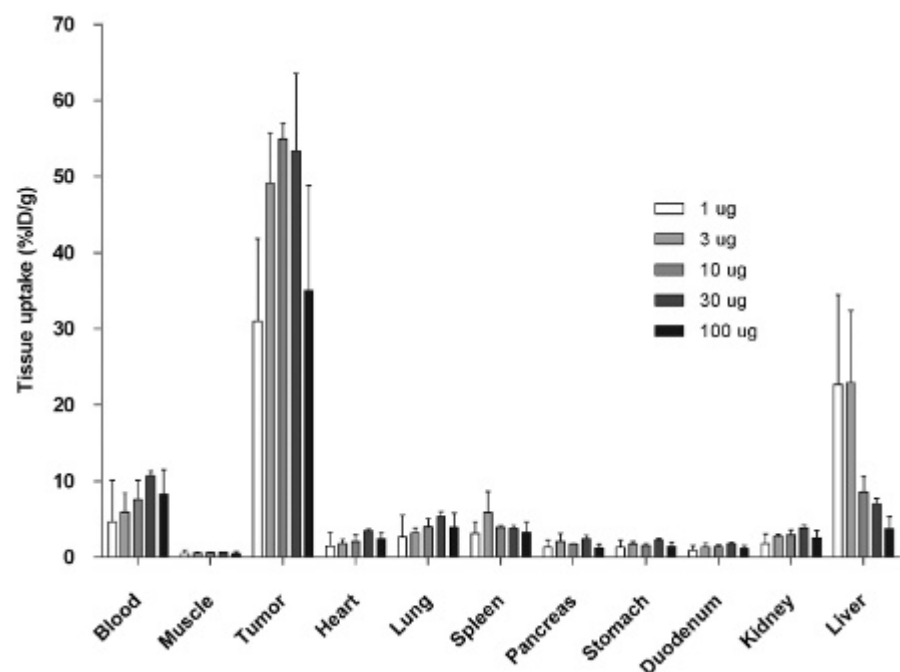


**Figure 2.** Biodistribution and specific tumor targeting of escalating doses of  $^{111}\text{In}$ -DTPA-G250 48 hours after injection. Tissue uptake is expressed as %ID/g. Values represent mean  $\pm$  standard deviation. Note the high liver uptake in the 1 and 3  $\mu\text{g}$  groups.



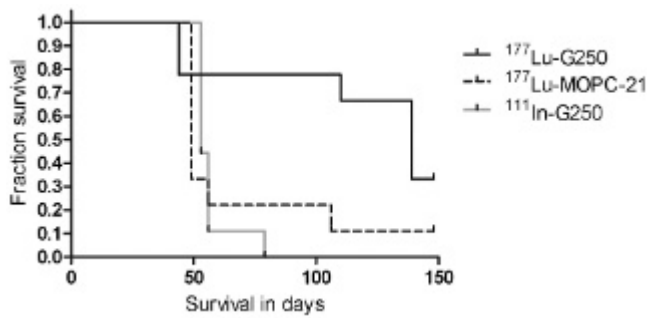


**Figure 3.** Kaplan-Meier survival estimates for the three groups in the radioimmunotherapy experiment. Treatment with  $^{177}\text{Lu}$ -DOTA-G250 resulted in significantly prolonged median survival of 139 days, in comparison with 49 days ( $^{177}\text{Lu}$ -DOTA-MOPC21) and 53 days of  $^{111}\text{In}$ -DOTA-G250 (Mantel-Cox  $p = .015$ ).

xenograft model was evaluated. The intraperitoneal model with the SK-RC-52 cell line proved reliable and highly reproducible as substantial tumor growth was established in the vast majority of the inoculated mice (in approximately 85%).

Several studies indicate that substantial differences in blood supply and physiology exist within different tumor models.<sup>14,15</sup> In the current study, we opted for intraperitoneally growing tumor nodules to more closely mimic metastatic disease with smaller tumor depositions in comparison with subcutaneous xenografts. The drawbacks of intraperitoneal tumor growth are that the lesions are not palpable the first weeks after induction and that

straightforward visual monitoring of the tumor growth is not possible. This makes *in vivo* imaging techniques indispensable if longitudinal quantification of tumor burden is required.

In the protein dose escalation study to determine the optimal antibody dose for *in vivo* targeting of the intraperitoneal ccRCC xenografts, mice did not show clinical signs of discomfort 3 weeks after inoculation of the SK-RC-52 tumor cells, nor were the intraperitoneally growing tumors palpable. Despite the small size of the intraperitoneal tumors, small depositions of approximately 1 to 2 mm and larger were well visualized with SPECT/CT 48 hours postinjection of  $^{111}\text{In}$ -DTPA-G250, emphasizing the specific and high accumulation of mAb G250. No clear differences in image quality between the different dose levels were observed. Due to the low protein and radiation dose administered, it is highly unlikely that multiple  $^{111}\text{In}$ -DTPA-G250 injections used for disease monitoring will have any effect on tumor progression.

The protein dose escalation experiment demonstrated that optimal T/B ratios and low liver uptake levels were reached at a protein dose of 10  $\mu\text{g}$ . Very high liver and low blood levels were observed in the animals with normal tumor load after 3 weeks in the 1 and 3  $\mu\text{g}$  groups. The mAb G250 biodistribution in the animals without any tumor depositions in these low-protein dose groups was similar to that in the 10, 30, and 100  $\mu\text{g}$  groups (data not shown). This suggests that the antibody distribution at low protein doses is heavily influenced by the presence of tumor. An inverse

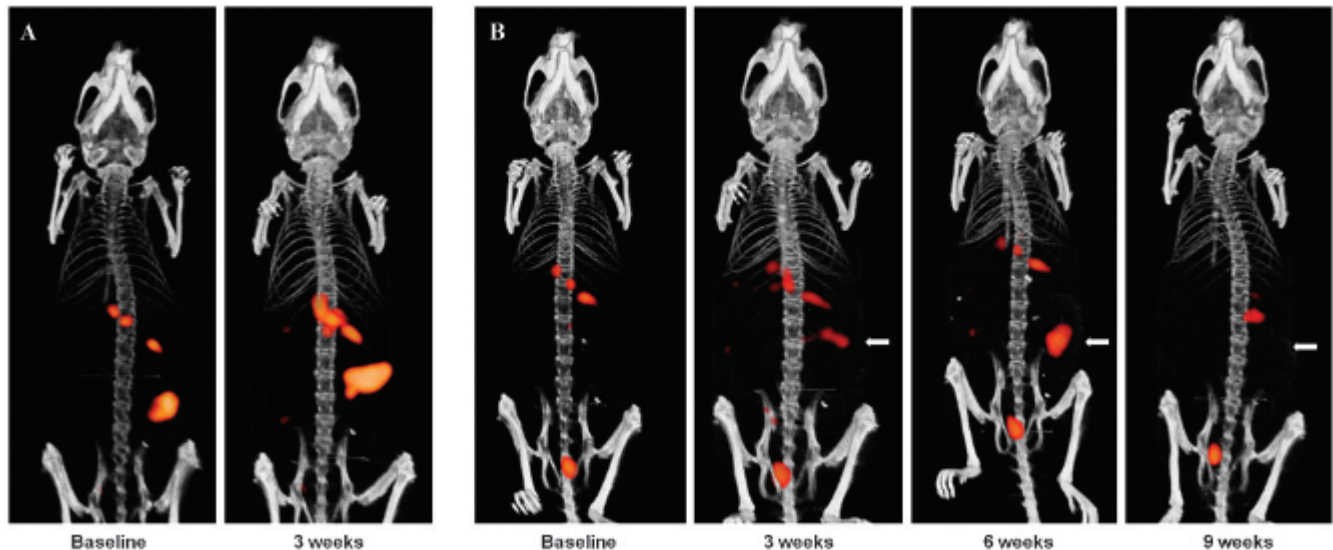


**Figure 4.** *In vivo* SPECT/CT imaging of mice with intraperitoneal clear cell renal cell carcinoma tumors. Rapid disease progression occurred in an animal in the  $^{111}\text{In}$ -DOTA-G250 group, which reached a humane end point after 5 weeks (A). Another animal was treated with  $^{177}\text{Lu}$ -DOTA-G250 immediately after baseline imaging (B). Note the presence and progression of a tumor in the left side of the abdomen after 3 and 6 weeks (arrows). The tumor was not detected with SPECT/CT after 9 weeks, was not found during dissection, and possibly regressed due to radioimmunotherapy.

correlation was observed between blood levels and liver uptake at the lower protein doses. This correlation could be the result of binding of  $^{111}\text{In}$ -DTPA-G250 to circulating antigen in the blood due to antigen shedding by the tumor,<sup>19</sup> which will lead to rapid clearance of the antibody-antigen immune complex via the liver, although we have no formal evidence of circulating antigen.

An additional advantage of an antibody dose of 10  $\mu\text{g}$  or more is that it is easier to label the antibody with higher doses of radioactivity, which are required for RIT. In the subsequent RIT study, we found a significantly prolonged median survival in the group treated with  $^{177}\text{Lu}$ -DOTA-G250. The difference in median survival in this study (139 days) and our previous results in a subcutaneous model (300 days)<sup>10</sup> is likely due to the location of the tumor depositions as the intraperitoneal tumors often result in obstruction of the gastrointestinal tract, which subsequently leads to rapid weight loss and clinical deterioration of the animals. In both models,  $^{177}\text{Lu}$ -DOTA-G250 clearly shows therapeutic potential.

Recently, several clinical studies reported severely hampered antibody targeting when radiolabeled antibodies were administered during TKI treatment.<sup>12,20</sup> To successfully combine TKI treatment and RIT in the future, additional preclinical studies are warranted to investigate the optimal sequence and timing of both treatment modalities. The intraperitoneal ccRCC xenograft model used in current study mimics metastatic ccRCC and is therefore suitable for future experiments, for instance, to determine for how long antibody targeting to the tumor is reduced after cessation of the TKI treatment. Better understanding of underlying mechanisms could be an important step in the development of successful RIT strategies for ccRCC.

## Acknowledgments

We thank Lieke Claessens-Joosten, Annemarie Eek, Hanneke Peeters, Bianca Lemmers-van de Weem, and Henk Arnts for their technical assistance.

Financial disclosure of authors: P.F.A. Mulders, W.J.G. Oyen, O.C. Boerman, and E. Oosterwijk serve(d) on an advisory board for Willex AG, Munich, Germany.

Financial disclosure of reviewers: None reported.

## References

1. Motzer RJ, Hutson TE, Tomczak P, et al. Sunitinib versus interferon alfa in metastatic renal-cell carcinoma. *N Engl J Med* 2007;356:115–24, doi:[10.1056/NEJMoa065044](#).
2. Sternberg CN, Davis ID, Mardiak J, et al. Pazopanib in locally advanced or metastatic renal cell carcinoma: results of a randomized phase III trial. *J Clin Oncol* 2010;28:1061–8, doi:[10.1200/JCO.2009.23.9764](#).
3. Escudier B, Pluzanska A, Koralewski P, et al. Bevacizumab plus interferon alfa-2a for treatment of metastatic renal cell carcinoma: a randomised, double-blind phase III trial. *Lancet* 2007;370:2103–11, doi:[10.1016/S0140-6736\(07\)61904-7](#).
4. Rini BI, Halabi S, Rosenberg JE, et al. Phase III trial of bevacizumab plus interferon alfa versus interferon alfa monotherapy in patients with metastatic renal cell carcinoma: final results of CALGB 90206. *J Clin Oncol* 2010;28:2137–43, doi:[10.1200/JCO.2009.26.5561](#).
5. Hudes G, Carducci M, Tomczak P, et al. Temsirolimus, interferon alfa, or both for advanced renal-cell carcinoma. *N Engl J Med* 2007;356:2271–81, doi:[10.1056/NEJMoa066838](#).
6. Hartmann JT, Haap M, Kopp H-G, et al. Tyrosine kinase inhibitors - a review on pharmacology, metabolism and side effects. *Curr Drug Metab* 2009;10:470–81, doi:[10.2174/138920009788897975](#).
7. Desar IM, Mulder SF, Stillebroer AB, et al. The reverse side of the victory: flare up of symptoms after discontinuation of sunitinib or sorafenib in renal cell cancer patients. A report of three cases. *Acta Oncol* 2009;48:927–31, doi:[10.1080/02841860902974167](#).
8. Leibovich BC, Sheinin Y, Lohse CM, et al. Carbonic anhydrase IX is not an independent predictor of outcome for patients with clear cell renal cell carcinoma. *J Clin Oncol* 2007;25:4757–64, doi:[10.1200/JCO.2007.12.1087](#).
9. Muselaers S, Mulders P, Oosterwijk E, et al. Molecular imaging and carbonic anhydrase IX-targeted radioimmunotherapy in clear cell renal cell carcinoma. *Immunotherapy* 2013;5:489–95, doi:[10.2217/imt.13.36](#).
10. Brouwers AH, van Eerd JE, Frielink C, et al. Optimization of radioimmunotherapy of renal cell carcinoma: labeling of monoclonal antibody cG250 with  $^{131}\text{I}$ ,  $^{90}\text{Y}$ ,  $^{177}\text{Lu}$ , or  $^{186}\text{Re}$ . *J Nucl Med* 2004;45:327–37.
11. Stillebroer AB, Boerman OC, Desar IM, et al. Phase 1 radioimmunotherapy study with lutetium  $^{177}$ -labeled anti-carbonic anhydrase IX monoclonal antibody girentuximab in patients with advanced renal cell carcinoma. *Eur Urol* 2013;64:478–85, doi:[10.1016/j.eururo.2012.08.024](#).
12. Muselaers CH, Stillebroer AB, Desar IM, et al. Tyrosine kinase inhibitor sorafenib decreases  $^{111}\text{In}$ -girentuximab uptake in patients with clear cell renal cell carcinoma. *J Nucl Med* 2014;55:242–7.
13. Oosterwijk-Wakka JC, Kats-Ugurlu G, Leenders WP, et al. Effect of tyrosine kinase inhibitor treatment of renal cell carcinoma on the accumulation of carbonic anhydrase IX-specific chimeric monoclonal antibody cG250. *BJU Int* 2011;107:118–25, doi:[10.1111/j.1464-410X.2010.09314.x](#).
14. Blumenthal RD, Sharkey RM, Kashi R, et al. Influence of animal host and tumor implantation site on radio-antibody uptake in the GW-39 human colonic cancer xenograft. *Int J Cancer* 1989;44:1041–7, doi:[10.1002/ijc.2910440617](#).
15. Hagan PL, Halpern SE, Dillman RO, et al. Tumor size: effect on monoclonal antibody uptake in tumor models. *J Nucl Med* 1986;27:422–7.
16. Brom M, Joosten L, Oven WJ, et al. Improved labelling of DTPA- and DOTA-conjugated peptides and antibodies with  $^{111}\text{In}$  in HEPES and MES buffer. *EJNMMI Res* 2012;2:4, doi:[10.1186/2191-219X-2-4](#).

- 
17. Lewis MR, Raubitschek A, Shively JE. A facile, water-soluble method for modification of proteins with DOTA. Use of elevated temperature and optimized pH to achieve high specific activity and high chelate stability in radiolabeled immunoconjugates. *Bioconjug Chem* 1994;5:565–76, doi:[10.1021/bc00030a012](https://doi.org/10.1021/bc00030a012).
  18. Ebert T, Bander NH, Finstad CL, et al. Establishment and characterization of human renal cancer and normal kidney cell lines. *Cancer Res* 1990;50:5531–6.
  19. Schuhmacher J, Kaul S, Klivenyi G, et al. Immunoscintigraphy with positron emission tomography: gallium-68 chelate imaging of breast cancer pretargeted with bispecific anti-MUC1/anti-Ga chelate antibodies. *Cancer Res* 2001;61:3712–7.
  20. Desar IM, Stillebroer AB, Oosterwijk E, et al. <sup>111</sup>In-bevacizumab imaging of renal cell cancer and evaluation of neoadjuvant treatment with the vascular endothelial growth factor receptor inhibitor sorafenib. *J Nucl Med* 2010;51:1707–15, doi:[10.2967/jnumed.110.078030](https://doi.org/10.2967/jnumed.110.078030).